Lawrence Berkeley National Laboratory

Title
MESON MASS MEASUREMENTS III. THE PI-MU MASS RATIO AND ENERGY BALANCE IN PION DECAY

Permalink
https://escholarship.org/uc/item/3924w1b4

Author
Birnbaum, Wallace.

Publication Date
1954-03-23

UNIVERSITY OF CALIFORNIA

Radiation Laboratory

BERKELEY, CALIFORNIA

UNIVERSITY OF CALIFORNIA

Radiation Laboratory

MESON MASS MEASUREMENTS III
THE PI-MU MASS RATIO AND ENERGY BALANCE IN PION DECAY

Wallace Birnbaum

March 23, 1954

Berkeley, California

TABLE OF CONTENTS

MESON MASS MEASUREMENTS III
THE PI-MU MASS RATIO AND ENERGY BALANCE IN PION DECAY

Wallace Birnbaum

Radiation Laboratory, Department of Physics
University of California, Berkeley, California

March 23, 1954

ABSTRACT

The mass normalization method of measuring meson masses is extended to a determination of the positive pion-muon mass ratio. Ranges and momenta of the comparison particles produced in the 184-inch cyclotron are measured, employing the nuclear emulsion technique. The energetics of the $\pi \rightarrow \mu + \nu$ decay scheme are also studied in detail. From precise determinations of the absolute decay momentum, p_0, of the muon and the π/μ mass ratio, various meson mass and related experimental values are obtained: $m_\pi^+/m_\mu^+ = 1.321 \pm 0.002$; $p_0 = 29.80 \pm 0.07$ Mev/c; a new probable upper limit of the mass, m_ν, of the neutral decay particle of $\approx 6\text{-}7\ m_0$; and a muon center-of-mass kinetic energy of 4.12 ± 0.02 Mev. With the positive pion mass value of Paper II, the m_π^+/m_μ^+ ratio yields $m_\mu^+ = 206.9 \pm 0.4\ m_0$. The following values in parentheses are insensitive to m_ν and are evaluated assuming $m_\nu = 0$: $m_\pi^+ - m_\mu^+ = (66.41 \pm 0.07\ m_0)$; $m_\mu^+ = (206.9 \pm 0.2\ m_0)$ from Paper II and the mass difference; $m_\pi^+ = (273.5 \pm 1.2\ m_0)$ and $m_\mu^+ = (207.0 \pm 1.1\ m_0)$ derived solely from the pion-muon mass ratio and mass difference.

MESON MASS MEASUREMENTS III
THE PI-MU MASS RATIO AND ENERGY BALANCE IN PION DECAY[*]

Wallace Birnbaum[**]

Radiation Laboratory, Department of Physics
University of California, Berkeley, California

March 23, 1954

I. INTRODUCTION

This article constitutes the third of a series of three papers on the "direct" measurements of the meson masses by the "Hρ vs. Range" mass ratio method. The theoretical basis of the experiment has been discussed by Walter H. Barkas in Paper I[1] and we shall follow his analysis closely in subsequent sections. Paper II, written by Frances M. Smith[2], deals with the experimental details and final results of the pion-proton mass ratio, and includes an experimental study of range straggling in nuclear emulsions. Frequent references to these preceding papers are made below.

The study here reported is a logical extension of the pion-proton mass ratio technique. The positive pion and the positive muon are chosen as the two comparison particles and the meson mass ratio is determined. At the same time, a critical quantitative analysis is made of the energetics of the pion-muon decay scheme, $\pi \to \mu + \nu$. All of the mass and kinetic energy relations connected with the dynamics of the decay involve functions of the mass ratio and the center-of-mass momentum acquired by the muon at the time of creation. This phase of the work yields a new value for the positive $\pi - \mu$ mass difference, and a new estimate of the upper limit of the mass of the neutral particle (presumably a neutrino[3]) which is involved in the two-body decay.

II. THEORY OF THE EXPERIMENT

A. The Statistical Calculation of the Pion-Muon Mass Ratio

In a manner analogous to the derivation of Eq. 6, Paper I, one obtains for pions and muons of the same velocity the following basic relation:

$$\left(\frac{m_\pi}{m_\mu}\right)^{1-q} = \frac{R_\pi p_\pi^{-q}}{R_\mu p_\mu^{-q}} \tag{1}$$

where R_π and R_μ are the residual ranges of the particles in the nuclear emulsion, p_π and p_μ are the respective momenta of the two types of mesons, and q is the exponent in the range-momentum relation[4], $R = cp^q$. For the statistical treatment of the data, the distributions of the quantity R_p^{-q} (termed the "normalized range") are again studied as in Paper II.

If one employs the average value of observed empirical quantities R_{1p}^{-q} in Eq. 1, one obtains an apparent mass ratio a' defined by

$$a' = \frac{m_\pi}{m_\mu} = \left[\frac{\left\langle R_{1\pi}\, p_\pi^{-q}\right\rangle}{\left\langle R_{1\mu}\, p_\mu^{-q}\right\rangle}\right]^{\frac{1}{1-q}} \tag{2}$$

where $R_{1\pi}$ and $R_{1\mu}$ are the measured ranges in the nuclear emulsion detector, and p_π and p_μ are the apparent momenta of the mesons, assuming the target to be a point source. The specific details of the calculation of the momenta of the mesons following trochoidal orbits in the 184-inch cyclotron are presented in both Papers I and II. The relation be ween the true mass ratio a and the apparent ratio a' can be derived by including the effects of the finite target size, the finite area of the detector, and the Lewis correction[5] to the measured range. From the analysis of Sec. V - Paper I, one can derive the equation:

$$a = a' \left[1 + \frac{e_{1\pi} - e_{1\mu}}{q-1} + \frac{\omega_{q\pi} - \omega_{q\mu}}{q-1}\right] \tag{3}$$

In Eq. 3, the Lewis correction e_1 is equal to $\dfrac{1}{612\, M \ln 3780\, \beta^2}$

(M is the mass of the particle in units of proton mass, and $\beta = v/c$).
The finite target and detector effects are represented by ω_q.

If there are n_π observations of π mesons and n_μ observations of
μ mesons, the uncertainty in the true mass ratio is given by

$$\sigma_a^2 = \frac{a^2}{(q-1)^2} \left[\frac{\sigma_\pi^2}{n_\pi \left\langle R_{1\pi} P_\pi^{-q} \right\rangle^2} + \frac{\sigma_\mu^2}{n_\mu \left\langle R_{1\mu} P_\mu^{-q} \right\rangle^2} + \right.$$

$$\frac{\sigma_q^2}{4} \left(\frac{\sigma_{P_\pi}^2}{\left\langle p_\pi \right\rangle^2} - \frac{\sigma_{P_\mu}^2}{\left\langle p_\mu \right\rangle^2} - 2r \right)^2 +$$

$$\left. \frac{\sigma_s^2}{s^2} \left(\left\langle \sin^2 \gamma_{1\pi} \right\rangle - \left\langle \sin^2 \gamma_{1\mu} \right\rangle \right)^2 \right] \qquad (4)$$

where σ_π^2 and σ_μ^2 are the observed variances of the pion and muon
normalized range distributions; σ_q^2 and σ_s^2 denote the uncertainties
in the choices of the momentum exponent and the shrinkage factor of
the emulsion, respectively (see Sec. IV C - Paper I);

$$\frac{\sigma_{P_\pi}^2}{\left\langle P_\pi \right\rangle^2} \quad \text{and} \quad \frac{\sigma_{P_\mu}^2}{\left\langle P_\mu \right\rangle^2}$$

measure the width of the momentum intervals chosen for the two
particles; r is defined by $\frac{\left\langle p_\pi \right\rangle}{\left\langle p_\mu \right\rangle} \equiv a (1 + r)$; γ_1 is the angle between an
element of track and the plane of the emulsion before processing, and
$\left\langle \sin^2 \gamma_1 \right\rangle$ is the experimentally measured mean value of $\left\langle \sin^2 \gamma_1 \right\rangle$ along
the path.

B. The dynamics of Pion-Muon Decay

   1. Absolute Meson Masses and Related Quantities

   A careful study of the energy and momentum balance of the
assumed mode of pion decay, $\pi \to \mu + \nu$, not only tests the validity of
this assumption, but also yields accurate meson mass relations in
terms of certain observables. However, the process of decay involv-
ing the sudden acceleration of the newly created muon is necessarily
accompanied by a continuous soft-photon spectrum. This process is

the analogue of the inner bremsstrahlung accompanying nuclear beta decay[6]. Therefore, kinetic energies of the muon from zero to the full energy T_o are possible. Several authors[7] have obtained expressions for the probability distribution function P (T, ϵ) dTdϵ, where ϵ refers to the kinetic energy of the photon. Thus, if one integrates with respect to ϵ, one obtains the probability P (T) dT of the muon's possessing a kinetic energy lying between T and T + dT. The ratio of the probability of soft-photon decay to radiationless decay for T < 3.5 Mev is calculated to be $\approx$ 1.3-2.0 x 10^{-4}. Fry[8], examining anomalously short muon tracks which cannot be explained by a decay-in-flight analysis, has obtained an experimental value for this probability of (3.3 $\pm$ 1.6) x 10^{-4}, which is in agreement as to order of magnitude. In any event, the probability of obtaining a "low-energy" μ meson is very small. If one calculates the mean energy of the muon arising from the presence of the complete bremsstrahlung spectrum, it is found to be but a few hundred electron volts less than the radiationless value of $\approx$ 4 Mev. Furthermore, since no anomalously short-range tracks are included in the present analysis, the effect of the inner bremsstrahlung process is felt even less. This difference of a few hundred electron volts is too small to be detected in this study. Therefore, for the purposes of this discussion, the decay of the pion resolves itself into a simple two-body problem. Thus we may write the relativistic equations for the conservation of energy and momentum for a pion decaying while at rest as follows:

$$m_\pi c^2 = \sqrt{p_\mu^2 c^2 + m_\mu^2 c^4} + \sqrt{p_\nu^2 c^2 + m_\nu^2 c^4} =$$

$$m_\mu c^2 + T_\mu + m_\nu c^2 + T_\nu \qquad (5a)$$

$$p_\mu = p_\nu \qquad (5b)$$

For future clarity of notation we distinguish between the momentum p_μ of a μ meson coming from the target and entering the emulsion,

and the momentum p_o of the μ meson acquired at the instant of its creation. We shall also define $\alpha \equiv m_\pi/m_\mu$, $\beta \equiv m_\nu/m_\mu$.

a. Mass of Neutral Particle

$$m_\nu = m_\mu \left[\alpha^2 + 1 - 2\alpha \sqrt{1 + (p_o/m_\mu c)^2} \right]^{1/2} \tag{6}$$

One cannot hope by this experiment to obtain a value of the mass of the presumed neutrino with an accuracy comparable to that obtained in the beta-decay studies[9]. As shown in Eq. 6, the mass of the neutrino is a function of a large mass value multiplied by the difference between two comparatively large numbers. Figure 1 shows the sensitivity of the derived neutrino mass to small changes in α, p_o, and the muon mass. One can merely arrive at a new upper limit to the mass of the neutral particle and note if any inconsistencies exist in the presumed mode of decay.

On the other hand, certain quantities can be derived which are very insensitive to the mass of the neutrino if it is indeed quite small. Hence, assuming $m_\nu = 0$, we have several important relations.

b. The Pion-Muon Mass Difference

$$(m_\pi - m_\mu) c^2 = \frac{2\alpha}{\alpha+1} p_o c \tag{7}$$

As will be shown later in Section III, very high accuracy can be obtained in the estimate of the mass difference. This difference, coupled with the value of the mass ratio α, enables one to derive absolute values of the positive pion and muon masses, independent of any other comparison particle such as the proton.

c. Masses of the Muon and Pion

$$m_\mu c^2 = \frac{2\alpha}{\alpha^2-1} p_o c \tag{8a}$$

$$m_\pi c^2 = \frac{2\alpha^2}{\alpha^2-1} p_o c \tag{8b}$$

d. Kinetic Energy of the Muon

$$T_o = \frac{a-1}{a+1} \, p_o c \qquad\qquad (9a)$$

$$T_o = \frac{a-1}{2a^2} \, m_\pi c^2 \qquad\qquad (9b)$$

From the usual relativistic relations, one can also obtain a value of the kinetic energy where E_μ is the total energy of the muon, with no assumptions regarding the mass of the neutrino.

$$T_o = E_\mu - m_\mu c^2 = \sqrt{p_o^2 c^2 + m_\mu^2 c^4} - m_\mu c^2 \qquad\qquad (10)$$

2. The Absolute Muon Decay Momentum

The pertinent mass and kinetic-energy relations connected with the dynamics of the decay scheme are functions of the mass ratio a and the full decay momentum p_o. The details of determining a have been sketched in brief in Sec. II A, and we shall now concern our-selves with the evaluation of the other important parameter, p_o.

Those μ mesons entering the detector from the target no longer have their full decay energy, owing to small losses within the target. The μ mesons created within the emulsion, however, and expending their entire energy therein, lend themselves to this phase fo the study. These mesons will now be referred to as " μ-completes" with momen-tum p_o, while those muons coming from the target will be termed "ρ-mesons" with momentum p_μ.

Once again, we utilize the range-momentum relation and the mass normalization property. Two methods involving the fundamental Eq. 1 are employed to determine p_o.

In the first method, the μ-completes are to be compared with the target ρ-mesons. Therefore, $m_1 = m_2 = m_\mu$. In Eq. 1, let $p_1 = p_o$, and $p_2 = p_\mu$ with associated residual ranges R_o and R_μ, respectively. Solving for the absolute decay momentum, we get

$$p_o = \left[\frac{R_o}{R_\mu p_\mu^{-q}} \right]^{1/q} \tag{11}$$

Now, however, the determination of an absolute value for p_o requires an absolute measurement of the magnetic field of the cyclotron. As before, the velocities of the two sets of mesons are to be chosen as nearly equal as is possible and still have adequate statistics for the analysis. This is desirable in order that the uncertainty in q, once again, is not a significant source of error. Thus, by determining the mean range of the μ-completes and the absolute meson value of the normalized range, $\langle R_{1\mu} p_\mu^{-q} \rangle$, and introducing the finite target and detector effects, one obtains

$$p_o = \left[\frac{\langle R_o \rangle}{\langle R_{1\mu} p_\mu^{-q} \rangle} \right]^{1/q} \left[1 + \frac{e_{1\mu} - e_{1o}}{q} + \omega_{q\mu} \right] \tag{12}$$

for which the various parameters have already been defined.

If we define t by the relation $t \equiv \dfrac{\langle p_\mu \rangle - p_o}{p_o}$, where $\langle p_\mu \rangle$ is the mean momentum of the ρ-mesons that are selected from the detector for range measurements, the uncertainty in p_o may be expressed by

$$\frac{\sigma_{p_o}^2}{p_o^2} \equiv \frac{1}{q^2} \left\{ \frac{\sigma_{R_o}^2}{n_o \langle R_o \rangle^2} + \frac{\sigma_\mu^2}{n_\mu \langle R_{1\mu} p_\mu^{-q} \rangle^2} + \frac{\sigma_q^2}{4} \left(\frac{\sigma_{p_\mu}^2}{\langle p_\mu \rangle^2} + 2t \right)^2 + \right.$$

$$\left. \frac{\sigma_s^2}{s^2} \left[\langle \sin^2 \gamma_{1\mu} \rangle - \langle \sin^2 \gamma_{1o} \rangle \right]^2 \right\} + \frac{\sigma_H^2}{H^2} \tag{13}$$

where $\sigma_{R_o}^2$ is the observed variance or range straggling of n_o μ-complete events. The additional term, $\dfrac{\sigma_H^2}{H^2}$, represents the uncertainty in the magnitude of the absolute value of the magnetic field.

In the second method, the mean range and momentum of the μ-completes are compared with the ranges and absolute momenta of

π mesons originating at the target and entering the emulsion detector. Once again the velocities of the two particles are to be chosen approximately equal. Applying the fundamental Eq. 1 we solve for p_o, obtaining

$$p_o = \left[\frac{\langle R_o \rangle}{a^{q-1} \langle R_{1_\pi} p_\pi^{-q} \rangle} \right]^{\frac{1}{q}} \left[1 + \frac{e_{1_\pi} - e_{1_o}}{q} + \frac{\omega_{q_\pi}}{q} \right] \quad (14)$$

Thus, knowing the value of the mass ratio a from an independent study, we have another method of evaluating the absolute decay momentum of the muon. If we take $\frac{\langle p_\pi \rangle}{p_o} \equiv a (1 - \delta)$ we now express the uncertainty in p_o as follows:

$$\frac{\sigma_{p_o}^2}{p_o^2} = \frac{1}{q^2} \left\{ \frac{\sigma_{R_o}^2}{n_o \langle R_o \rangle^2} + \frac{\sigma_\pi^2}{n_\pi \langle R_{1_\pi} p_\pi^{-q} \rangle^2} + \right.$$

$$(1 - q)^2 \frac{\sigma_a^2}{a^2} + \frac{\sigma_q^2}{4} \left(\frac{\sigma_{p_\pi}^2}{\langle p_\pi \rangle^2} + 2\delta \right)^2 +$$

$$\left. \frac{\sigma_s^2}{s^2} \left[\langle \sin^2 \gamma_{1_\pi} \rangle - \langle \sin^2 \gamma_{1_o} \rangle \right]^2 \right\} + \frac{\sigma_H^2}{H^2} \quad (15)$$

where σ_a^2 is the uncertainty in the value of the π/μ mass ratio.

III. EXPERIMENTAL TECHNIQUES

A. Geometrical Arrangement

1. Exposures Within the Cyclotron

The mesons under study are produced by the internal circulating proton beam of the 184-inch cyclotron. The geometrical arrangement is shown schematically in Fig. 2. The protons (≈ 290 Mev) strike a thin copper target, producing π mesons. Those positive pions leaving the target with energies acceptable to the defining channel spiral down under the influence of the cyclotron magnetic field and enter a 200 micron thick Ilford C-2 nuclear-emulsion detector. The points of entry of the

pions are distributed more or less uniformly over the entire plate.

At the same time, positive pions coming to rest within the target decay into muons. Those muons created near the surface of the target leave with only small energy losses and can be accepted by the channel if their angles of emission are "proper", entering the emulsion in a more defined region of the plate. The pions reaching the detector lose energy and stop within the emulsion, giving rise to muons, approximately 17 percent of which come to the end of their range before leaving the plate. These μ mesons have previously been referred to as the "μ-completes". The target muons or "ρ-mesons" coming to rest decay into an electron plus two neutrinos. Since the C-2 emulsion is insensitive to electrons, one can quickly distinguish between a pion and a muon by simply observing whether or not another track appears at the end of the range of the particle.

Previous estimates of the π/μ mass ratio indicated a value of ≈ 1.3. In order to establish the equal-velocity criterion and thereby minimize the effects of any uncertainty in q, the energy chosen for the pions is ≈ 5.2 Mev to allow comparison with the ρ-mesons and μ-completes of ≈ 4 Mev. Theoretically, one could utilize the concept of "successive approximations"[*] and repeat this procedure several times, each successive analysis converging closer to the ideal condition of exactly equal velocities for the two comparison particles. In this experiment, the initial momentum intervals chosen are such that the uncertainty in the momentum exponent ($q = 3.44 \pm 0.03$) has an essentially negligible effect in the final determination of the mass ratio. Hence, further narrowing of the momentum intervals is unnecessary.

The experimental apparatus is mounted on a cart and run into the main vacuum tank of the cyclotron by means of the so-called "proton probe". The cart is stopped along its track at a point that places the meson target at a cyclotron radius of 73 inches. This is the maximum allowable radius at which the trajectories of the particles under study remain within the fairly uniform region of the magnetic field; the diameters of the pion orbits are approximately seven inches. Figure 7 gives the magnetic field intensity as a function of cyclotron radius, showing the change in slope at the 80-inch point.

---

[*]The application of the successive-approximations concept to this study was first suggested by E. Gardner.[10]

2. Target and Detector Assembly

A perspective sketch showing the arrangement of the target, channel, and detector plate is presented in Fig. 3. The entire apparatus is mounted and fixed upon a dural base and later placed on the proton probe cart. Considerable care is given to the establishment of a median reference line (termed the Central Radial Line) passing through the centers of the target and plate holder.

In the first set of exposures, Run I, the meson target of copper had the dimensions 0.041" x 1/4" x 1/2" and was attached to a narrow copper stem. To increase the solid angle, the target center was located at a height of 0.44 ± 0.06 inches above the surface of the emulsion. A wedge-shaped carbon absorber was placed in the channel, effectively casting a geometrical shadow and preventing mesons that originated in the stem from reaching the detector.

In a subsequent experimental run, Run II, the mounting of the 40-mil target was improved (see Fig. 4). The experimental arrangement of Run II (the second π^+/p run of Paper II) is described in detail by Frances Smith. The experimental arrangement for accepting target pions in the detector was essentially the same as in Run I, except for the "major" modification in the target assembly. The need of a shadow in the channel was eliminated, since the contributions from the 1-mil tungsten wires supporting the target were negligible.

It was desirable to have uniform irradiation of the target to facilitate the identification of the effective geometric center of the meson production. Consequently, preliminary tests were made to locate the median plane of the circulating proton beam as well as its intensity half-width in the vertical direction. Bowker[11], employing thin polyethlene monitors, has measured the vertical profile of the beam. Readings of the activity from the $C^{12}(p, pn) C^{11}$ reaction with the aid of a Lauritsen electroscope indicated that the beam intensity drops to half maximum in a vertical distance of 0.25 inch. The median plane of the beam was also checked by irradiating a 3-inch long graphite cylinder of 36-mil diameter and locating the point of maximum activity. At the 73-inch radius, it was found to be ≈ 0.25 inch below the median plane of the gap between the pole faces of the cyclotron magnet. A mock target, consisting of four 10-mil slices pressed

together, was bombarded to check the relative irradiation across the target by the beam. All four sections, when separated, showed essentially the same activity.

The original philosophy regarding the channel was to have the minimum amount of shielding that appeared feasible. Background problems inside the vacuum tank of the cyclotron are rather severe and ordinarily call for considerable shielding. On the other hand, using a great deal of shielding can increase the possibility of contamination from mesons scattering off the channel walls. Preliminary runs were made with wide-open channels and comparatively little shielding. Exposures had to be limited to 10 seconds to prevent the heavy neutron-proton background from completely obscuring the desired mesons; consequently, statistics were poor. Moreover, as the plates were placed in the apparatus without any outer paper wrapping, any source of light within the tank could blacken the film surfaces. Arcing from the dee, and light emanating from the tungsten filament in the cyclotron ion course, clearly indicated the need of some light shielding.

Therefore, the final channel of Run I represents the inevitable compromise. More shielding is employed to permit increased exposure times (30-45 seconds) and to decrease the ever present light hazards. The channel is designed to accept mesons leaving the target within specified angular intervals (π mesons with the angles in the backward direction with respect to the incident proton beam of $\pm 10^{\circ}$ and ρ-mesons with angles of -15° to $+ 10^{\circ}$). Production of mesons in the shielding by protons and the scattering of target mesons in the channel are effectively minimized. The channel was shaped empirically, drawing meson trajectories from all points of the channel. Any unwanted meson that did manage to get through would either have entered the detector with the wrong angle or would have had a considerably lower or higher energy and consequently could then easily be separated from the main distribution by its range measurement. The copper walls are lined with 1/8-inch polyethylene to lower the atomic number of the surface material and thereby possibly reduce the scattering. A certain amount of decay in flight is present that cannot be prevented from reaching the detector. This effect, however, is small, as is seen in the ρ-meson distributions obtained.

The detector is mounted on a 1 x 3-inch plate holder having an inclination angle of 5° with respect to the horizontal x-y plane. The type of plate holder is shown in Fig. 5. A glass-backed photographic film negative of a drawing of two fiducial marks is cemented on the surface of the holder. The Central Radial Line joining the centers of the fiducial marks, when extended, passes through the center of the target. By means of a small battery-operated lamp a latent image of these fiducial lines is produced in the nuclear emulsion detector after it has been fixed on top of the negative by phosphor bronze clamps. These lines not only give a permanent record of the exact position of the detector at the time of exposure, but also enable the investigator to locate quickly the proper regions of the plate to be scanned under the microscope (i. e., momentum intervals which give approximately equal velocities for the pion and muon, respectively). At the time of exposure a brass measuring bar is laid parallel to the reference Central Radial Line and the distances between the target and the fiducial marks are readily determined with the aid of a low-power microscope attached to a micrometer. The brass bar contains two fiducial marks whose known distance apart is approximately equal to the target-detector distance. Hence, one then measures small differerences between the target and the first bar mark, and between the plate holder fiducial lines and the second bar mark. Figure 6 shows schematically the actual physical measurements made for Run I. The differences can be read to 0.1 mil, and the overall distance between the center of the target and the plate fiducial mark is probably known to one mil. This represents a negligible contribution to the total uncertainty in the final momentum determination.

In the calculation of the momentum, it should be emphasized that the locations of the target and detector are considered with reference to two coordinate systems. The first reference frame has its origin at the center of the target. In this frame, the distance between the target and detector is known to high accuracy ($\approx$ 1 part in 10^{4}), and the entire target-detector assembly remains fixed on its dural base for a particular run. The percentage error in the target-detector distance

reflects itself directly as an equal uncertainty in the momentum. The second frame of reference has its origin at the center of the cyclotron, for the absolute value of the magnetic field is known as a function of the cyclotron radius. The proton probe cart carrying the target-detector assembly can be set at any desired radius to an accuracy of $\approx 1/8$ inch. Since the gradient of the field in this region is ≈ 10 gausses per inch, the error in the location of the cart gives an error in the momentum of less than one part in 10^4. This error is an order of magnitude smaller than the overall uncertainty in the actual measurement of the field itself.

B. Criteria for Acceptance of an Event

The microscope techniques employed in measuring the angle of entrance θ of the particle at the surface of the emulsion, and the determination of the residual range R_1, have been described in Paper II. The accuracy of the determination of the absolute value of θ as measured with the aid of an eyepiece reticle and external protractor (goniometer) is estimated at $\pm 1^{\circ}$. Therefore the angular requirements for mesons accepted for range measurement are $\theta' = -11^{\circ}$ to $+11^{\circ}$ for pions, and $\theta' = -15^{\circ}$ to $+11^{\circ}$ for muons. Here θ' is defined as the angle a track makes with the normal (y-axis) to the Central Raidal Line (x-axis) of the target-detector assembly if its orbit is extended until it crosses the x-axis. For these orbits in the slowly varying magnetic field of the cyclotron, the magnitude of the precession angle is approximately ten minutes and may be neglected. Thus θ' also represents the angle of emission at the target of the detected mesons.

Another criterion for acceptance by the microscope observer involves the dip angle of the track at the surface of the emulsion. The expected dip angle for a particle leaving the target is easily calculated from the geometry of the target-detector assembly. Both the dip angle and range measurements require a calibration of the fine-focus adjustment of the microscope (vertical z-motion) and a knowledge of the shrinkage factor S of the emulsion[12]. The calibration is accomplished by measuring the known thickness of a thin cover glass. Because of the shrinkage factor and the rather small angles involved, accurate

measurements of the dip are not possible. As the amount of scatter-
ing of these low-energy mesons within the emulsion is large, only
short track lengths in the x-y plane can be considered. The tangent of
the dip angle is then determined by measuring the change in depth of the
track over this short segment of length. Mesons are accepted for anal-
ysis with observed dip angles lying within a 5°-9° interval.

C. Magnetic Measurements

Absolute measurements of the magnetic field are carried out with
the aid of the nuclear induction technique[13], employing the Varian Asso-
ciates Nuclear Induction Meter. In the preliminary runs, the proton-
moment head, containing the water sample and coils, was mounted
directly on top of the channel, and the Larmor frequency was measured
at the same time as the plate exposure. Because of certain engineering
difficulties, this arrangement proved to be too cumbersome for efficient
operation. The absolute values of the preliminary determinations of the
magnetic field intensity (for the same excitation current) were found,
on different days, to be equal to each other within a few gausses. This
is not particularly surprising, as the magnet is operating near satura-
tion; hence, hysteresis effects are expected to be small. Consequently,
a more efficient procedure was adopted. In Run I exposures were made
on one day, and the cyclotron field was measured the following day,
carefully monitoring the field current by means of a Leeds-Northrup
potentiometer. In Run II both the exposures and the field measurements
were completed in the same day, but not simultaneously. The proton-
moment head was inserted into the cyclotron by means of a special
probe at the conclusion of the plate exposures.

Figure 7 shows a plot of several determinations of the absolute
field as a function of cyclotron radius. In all cases the magnetic field
currents had been set for 5 to 6 hours. The individual values obtained
all fall within ± 0.1 percent of the mean value despite the widely different
dates of the measurements. The Larmor frequency, and therefore the
value of the field, can be located on an oscilloscope and read on a
General Radio signal generator to $\approx$ 0.03 percent accuracy for any one
determination.

Because the field measurements were not taken simultaneously
with the actual exposures, the uncertainties in the absolute values of
the magnetic fields are conservatively estimated at ± 0.1 percent
(standard error) for Run II, and ± 0.2 percent for Run I, after com-
pounding the various sources of possible error.

IV. ANALYSIS OF EXPERIMENTAL DATA

A. Range Straggling of the Mu-Completes

Since the main source of variance in the R_p^{-q} distribution func-
tion originates from the range straggling, this effect has been studied
experimentally in some detail by Frances Smith in Paper II. Data have
been taken from twelve plates adding up to a total of 558 μ-complete
events. Since the stopping power varies from one emulsion to another,
it was necessary to normalize the individual mean range values of each
plate to an arbitrary value of 600 microns when the data were combined
together. The entire distribution is plotted in Fig. 8. The percentage
standard deviation of this distribution is found to be equal to 4.5 ± 0.1.
The statistical estimate of the skewness indicates a slight but not sta-
tistically significant deviation from a true Gaussian distribution.

B. The Normalized Range Distribution Functions

The range variance obtained for the μ-completes serves as a
calibration function for the various $R_1 p^{-q}$ distributions being studied.
The experiment is designed so that contributions to the total variance
of the normalized range distributions from the momentum spread of
the detected mesons is negligible. For two particles of equal veloci-
ties, if range straggling is the chief contributor to the variance of $R_1 p^{-q}$,
it is easily shown that the relative variances of the two normalized range
distributions are inversely proportional to their masses. Therefore,
one should expect for the target pions,

$$\frac{\sigma_\pi^2}{\langle R_{1_\pi} P_\pi^{-q} \rangle} \approx 4.0 \%$$

and for the target muons,

$$\frac{\sigma_\mu}{\left\langle R_{1_\mu} P_\mu^{-q} \right\rangle} \approx 4.5\%$$

Any significant increases above these values would indicate the presence of contamination.

Run I

In this run, the normalized ranges of the target pions and muons (ρ mesons) are compared to determine the mass ratio. In addition, a value for the absolute decay momentum is obtained by comparing the normalized ranges of the ρ mesons with the ranges of the μ-completes. The latter distributions are shown in Fig. 9.

The data for this run have been collected from five different plates. For simplicity, the constant multiplicative factor e/c has been omitted in the calculation of p_o . The π meson and ρ meson normalized range distributions are plotted in Figs. 10 and 11, with p actually representing the magnetic rigidity of the particles. In general, two distinct peaks are observed, corresponding to the two types of mesons coming from the target. A small amount of background contamination also appears to be present. Since a few of the background events run into the tails of the main distributions, the following procedure is employed:

(a) The median of the distribution is determined including all "questionable" events. The median is first chosen as a statistical measure, since it is less sensitive to spurious events than the mean, especially for small sample statistics.

(b) When the median has been determined, the theoretically expected standard deviations of

$$\frac{\sigma_\pi}{\left\langle R_{1_\pi} P_\pi^{-q} \right\rangle} = 4.0\% \quad \text{and} \quad \frac{\sigma_\mu}{\left\langle R_{1_\mu} P_\mu^{-q} \right\rangle} = 4.5\%$$

are "folded" into the distributions, and any events lying outside an interval of $\pm 3\sigma$ from the median are considered as background.

(c) The mean $\langle R_1 p^{-q} \rangle$ and its standard deviation are then calculated for the adjusted distribution as outlined in Sec. II A.

Table I includes the final $\langle R_1 p^{-q} \rangle$ results with the associated $\langle R_0 \rangle_i$. Actually, a total of only eight events (five π mesons and three ρ mesons) that are "questionable" are omitted from the final calculations. The average percentage straggling values for the normalized range distributions containing no "questionable" events are:

$$\frac{\sigma_\pi}{\langle R_{1_\pi} p_\pi^{-q} \rangle} = 3.8 \pm 0.2\% \quad \text{and} \quad \frac{\sigma_\mu}{\langle R_{1_\mu} p_\mu^{-q} \rangle} = 4.9 \pm 0.2\%$$

The deviations from predicted values are not considered statistically significant, although there is always the possibility that a small amount of indistinguishable contamination may lie within the $\pm 3\sigma$ interval. In the few cases where some events are eliminated, the computed standard deviations of the adjusted distributions also agree with the expected values, whereas the unadjusted distributions have standard deviations which are 50-60 percent larger due to the presence of the few spurious events.

The existence of the background is probably due to the presence of the carbon shadow absorber that was placed in the channel, as described in Sec. III A. Also, with the present geometry, the ρ meson distributions will always have ≈ 5 percent contamination originating from pions decaying in flight.

Run II

To test the possibility of unknown experimental systematic errors, especially in the measurement of the absolute value of the magnetic field, another set of exposures within the cyclotron was made. In this run, the normalized ranges of target pions were compared with the μ-complete ranges to obtain a value for the absolute decay momentum. The pion events studied in this run, aside from a few exceptions, are the same as those analyzed in the second π^+/ρ run of Paper II.

As described in Sec. III A, the target assembly was improved for this run, and the shadow absorber was also removed from the channel.

The $R_{1_\pi}p_\pi^{-q}$ distributions obtained are plotted in Fig. 12. One imme-
diately observes the absence of any apparent background in the distri-
butions. It is also of interest to note the comparative values of
$\langle R_{1_\pi}p_\pi^{-q}\rangle$ for the three plates. Whereas two (No. 28848 and No. 28853)
are essentially equal, the third (No. 28849) is considerably higher. A
comparison of the $\langle R_o\rangle$ associated with the μ-completes of the three
plates shows the same trend (Fig. 13). These results, which are also
summarized in Table I, emphasize the effectiveness of the mass nor-
malization method, illustrating the uncertainties that are present when
one employs an absolute range-energy relation. The observed standard
deviations are in excellent agreement with the predicted values, further
indicating the lack of contamination.

C. Derived Experimental Values

All errors to be quoted below in this section are statistical prob-
able errors.

1. The Pi-Mu Mass Ratio and the Mass of the Muon

As discussed in Sec. II B, the π/μ mass ratio, α, and absolute
decay momentum, p_o, are the fundamental experimental quantities.
Table II presents a summary of the calculation of the π/μ mass ratio
from Eqs. 3 and 4. The weighted average over the five plates of Run I
yields the following result:

$$\langle \alpha \rangle = 1.321 \pm 0.002.$$

The statistical probable error calculated from external consistency is
equal to ± 0.002, and from internal consistency is equal to ± 0.0017.[14]
These values give a ratio of 1.18 ± 0.22, indicating that no large sys-
tematic errors are present.

The Lewis Effect correction systematically lowered the apparent
mass ratio α' by ≈ 0.0003. The finite target-detector corrections vary
over the individual plates from -0.0025 to $+0.0015$. The largest con-
tributions, by far, to the total probable error come from the variances
of the observed normalized range distributions of $R_{1_\pi}p_\pi^{-q}$ and
$R_{1_\mu}p_\mu^{-q}$. The uncertainties introduced by the σ_q^2 and σ_S^2 terms are
only 10^{-3} as large.

The mass of the positive pion has been determined accurately and independently from Run I in Paper II and found to be equal to 273.3 ± 0.2 m_0 . (For future applications in this paper we shall refer to this estimate to the positive pion mass as the "Smith value".) Inserting the Smith value into our present estimate of the π/μ mass ratio, one obtains

$$m_\mu = 206.9 \pm 0.4\, m_0.$$

2. The Absolute Muon Decay Momentum

Table III gives a summary of the calculations of $(p_0)_I$ and $(p_0)_{II}$ employing Eqs. 12 and 13 for Run I, and Eqs. 14 and 15 for Run II, respectively.

The Lewis Effect correction is zero for Run I, since we are comparing equal mass particles (ρ mesons and μ-completes). The finite target detector corrections vary from - 0.02 to + 0.08 Mev/c over the five plates. In Run II, where one compares the μ-completes with target pions, the Lewis correction systematically lowers the apparent momentum by 0.006 Mev/c, whereas the finite target-detector corrections vary from - 0.006 to + 0.002 Mev/c. The ratio of external to internal consistency in Run I is equal to 1.18 ± 0.22; in Run II the ratio is equal to 0.70 ± 0.28. In Run I, the uncertainty in the absolute value of the magnetic field (see Sec. III C) is the dominant term in the probable error, with a smaller contribution from range straggling . In Run II, the error in the momentum calculation is determined by the uncertainty in α and the inherent range straggling, and to a lesser degree by the uncertainty in the magnetic field. The following values are obtained:

Run I: p_0 = 29.85 Mev/c,

Run II: p_0 = 29.77 Mev/c.

The values chosen for the physical constants needed to convert from units of gauss-mm to those of Mev/c are taken from the latest of DuMond and Cohen.[15]

As noted in Eq. 14, p_o is a function of α, which is determined from Run I. Therefore, since the determination of a mean value for p_o from both runs involves dependent quantities, a simple averaging of the two values is no longer valid. In general, the computations of final mean values for all the other pertinent quantities given below depend upon interrelated parameters. Hence, it is necessary in the averaging procedure and in the propagation of errors to express all the equations of Sec. II B only in terms of directly observable and independent quantities. The lengthy details of these calculations employing the Mothod of Least Squares are outlined in the Appendix. One obtains the weighted mean,

$$\langle p_o \rangle = 29.80 + 0.04 \text{ Mev/c}.$$

3. The Mass of the Neutral Decay Particle (Eq. 6)

If one employs the Method of Least Squares to calculate the weighted mean value for m_ν with its associated probable error, we are led to an extremely cumbersome algebraic expression. As is readily seen in Fig. 1, the derived mass of the presumed neutrino is extremely sensitive to slight variations in α, p_o, and m_μ. Therefore, because of the statistical uncertainties in the values of these parameters, the exact analytical solution is not attempted and a graphical method is applied. Higher accuracy is also achieved if one replaces m_μ in Eq. 6 by the quantity m_π/α, where m_π is the Smith value for the pion mass. The graphical solution is presented in Fig. 14. A family of curves for different values of β ($\equiv m_\nu/m_\mu$) can be plotted as a function of α and the quantity $p_o/m_\pi c$. The hatched region is the area subtended by their probable errors. If one substitutes the final weighted means given above for these parameters into Eq. 6, one finds $\beta^2 = 0.0001$, but with an error of ≈ 400-500 percent. Examination of Fig. 14 indicates a probable upper limit to the mass of the neutral decay particle of ≈ 6-7 m_o.

As mentioned previously in Sec. II B, certain mass relations are insensitive to the mass of the neutral decay particle if m_ν is small. Therefore, if we assume $m_\nu = 0$ we obtain the following results.

4. The Pi – Mu Mass Difference (Eq. 7) and the Mass of the Muon

Run I: $m_\pi^+ - m_\mu^+ = 66.53 \pm 0.10\ m_o$

Run II: $m_\pi^+ - m_\mu^+ = 66.32 \pm 0.10\ m_o$

Mean : $\langle m_\pi^+ - m_\mu^+ \rangle = 66.41 \pm 0.07\ m_o$

Introducing the Smith pion value into our final weighted mean value for the π-μ mass difference, we have

$$m_\mu^+ = 206.9 \pm 0.2\ m_o .$$

5. The Absolute Kinetic Energy of the Muon

Assuming $m_\nu = 0$, we have from Eq. 9(a)

Run I: $T_o = 4.126 \pm 0.017$ Mev

Run II: $T_o = 4.117 \pm 0.023$ Mev

Mean : $\langle T_o \rangle = 4.123 \pm 0.016$ Mev.

If we now substitute the Smith positive-pion value into Eq. 9(b) along with the value for the mass ratio, one obtains another estimate for the kinetic energy,

$$T_o = 4.123 \pm 0.038\ \text{Mev}.$$

One can also determine T_o from the usual relativistic energy-momentum mass relation, Eq. 10, with no assumptions being made about the mass of the neutrino. For the best estimate of the mass of the muon we again use the Smith pion mass value and divide by the mass ratio, a. However, as in the case for m_ν above, the Method of Least Squares leads to algebraic complications. The exact solution of this equation involves some rather lengthy calculations which appear to be unwarranted in view of the magnitudes of the statistical probable errors. Therefore, for simplicity, a graphical method is once again used to eliminate the tedious algebra. In Fig. 15 a family of curves for different values of T_o is plotted as a function of the muon mass and the absolute decay momentum. The hatched region represents the area subtended

by probable errors in m_μ and p_o. Although this is not a rigorous mathematical treatment of the problem, one certainly obtains a good estimate of T_o. The following value is found:

$$T_o = 4.12 \pm 0.02 \text{ Mev.}$$

6. Supplementary Estimates of the Absolute Muon and Pion Masses

If we again assume $m_\nu = 0$, from Eq. 8(a) we have

$$\text{Run I:} \quad m_\mu{}^+ = 207.2 \pm 1.2 \, m_o$$

$$\text{Run II:} \quad m_\mu{}^+ = 206.6 \pm 1.4 \, m_o$$

$$\text{Mean :} \quad \left\langle m_\mu{}^+ \right\rangle = 207.1 \pm 1.1 \, m_o$$

and from Eq. 8(b)

$$\text{Mean :} \quad \left\langle m_\pi{}^+ \right\rangle = 273.5 \pm 1.2 \, m_o \, .$$

V. CONCLUSIONS

The chief limitation to the experiment and largest contributor to the various probable errors has been the inherent range straggling of the particles traversing the nuclear emulsion medium.

The absolute positive pion value of $273.5 \pm 1.2 \, m_o$ derived here through assuming $m_\nu = 0$ is in excellent agreement with the value of $273.3 \pm 0.2 \, m_o$ found in Paper II. Employing the pion value of Paper II in conjunction with this study, one obtains $m_\mu{}^+ = 206.9 \pm 0.4 \, m_o$ from the π/μ mass ratio with no assumptions regarding the mass of the neutral decay particle; on the other hand, if one assumes $m_\nu = 0$, then one gets $m_\mu{}^+ = 206.9 \pm 0.2 \, m_o$ from the calculated mass difference. Finally, from the mass ratio and the mass difference alone, we obtain $m_\mu{}^+ = 207.1 \pm 1.1 \, m_o$, further indicating quantitatively that the assumed decay scheme probably involves neutrino.

Several theories of meson masses have been advanced in the past few years by different authors. Because present-day theoreticians have not come to any definite conclusions in their efforts to explain the mass spectrum and its role in the theory of nuclear forces, no attempt has been made to relate the results of this study with nuclear theory.

ACKNOWLEDGEMENTS

APPENDIX

The Averaging Procedure and the Propagation of Errors

The π/μ mass ratio a is determined solely from Run I with an uncertainty expressed by Eq. 4. The relative magnitudes fo the terms contributing to the total error in a are such that uncertainties introduced by the σ_s^2 and σ_q^2 terms are essentially negligible. Therefore, in the following discussion, those terms which are functions of σ_s^2 and σ_q^2 will be omitted for the purpose of simplicity.

Unlike the value of a, all other experimental values are averaged over both Runs I and II. Since the individual means obtained from each of the runs are not completely independent of each other, the usual simple averaging procedure is no longer valid. It is therefore necessary to express all the pertinent equations of Sec. II B in terms of directly observable and independent paramenters.

The following detailed analysis gives a sample of the procedure employed in obtaining final mean values for the meson masses and their related quantities.

In Run I, the absolute momentum p_o is determined from the relation:

$$(p_o)_I = \left[\frac{\langle R_o \rangle}{\langle R_{1_\mu} p_\mu^{-q} \rangle} \right]^{\frac{1}{q}} \left[1 + \frac{e_{1_\mu} - e_{1_o}}{q} + \frac{\omega_{q_\mu}}{q} \right] \quad (12)$$

In Run II,

$$(p_o)_{II} = \left[\frac{\langle R_o' \rangle}{a^{q-1} \langle R_{1_\pi'} p_\pi'^{-q} \rangle} \right]^{\frac{1}{q}} \left[1 + \frac{e_{1_\pi}' - e_{1_o}'}{q} + \frac{\omega_{q_\pi}'}{q} \right] \quad (14)$$

As the terms in e and ω_q are quite small, they can be neglected in the present discussion. The primed measurable quantities refer to Run II; the unprimed to Run I. It is to be noted in Eq. 14 that $(p_o)_{II}$ is a function of a, which has been determined from Run I. Since

$$a \approx \left[\frac{\langle R_{1_\pi} p_\pi^{-q} \rangle}{\langle R_{1_\mu} p_\mu^{-q} \rangle} \right]^{\frac{1}{1-q}} \quad (2)$$

we may rewrite Eq. 14 as follows:

$$(p_o)_{II} = \left[\frac{\langle R_o' \rangle}{\langle R_{1_\pi'} p_\pi'^{-q} \rangle} \right]^{\frac{1}{q}} \left[\frac{\langle R_{1_\pi} p_\pi^{-q} \rangle}{\langle R_{1_\mu} p_\mu^{-q} \rangle} \right]^{\frac{1}{q}} \qquad (A.1)$$

We shall choose the calculation of the pion-muon mass difference to serve as a typical example of the general averaging procedure followed.

$$(m_\pi - m_\mu) c^2 = \frac{2a}{a+1} p_o c \qquad (7)$$

For simplicity of notation, let $\lambda = (m_\pi - m_\mu) c^2$, $\langle K_\pi \rangle = \langle R_{1_\pi} p_\pi^{-q} \rangle$ and $\langle K_\mu \rangle = \langle R_{1_\mu} p_\mu^{-q} \rangle$. Therefore, for Runs I and II, we may write Eq. 7 in terms of observable quantities:

$$\lambda_I = \frac{2c \left[\frac{\langle K_\pi \rangle}{\langle K_\mu \rangle} \right]^{\frac{1}{1-q}}}{\left[\frac{\langle K_\pi \rangle}{\langle K_\mu \rangle} \right]^{\frac{1}{1-q}} + 1} \left[\frac{\langle R_o \rangle}{\langle K_\mu \rangle} \right]^{\frac{1}{q}} \qquad (A.2a)$$

and

$$\lambda_{II} = \frac{2c \left[\frac{\langle K_\pi \rangle}{\langle K_\mu \rangle} \right]^{\frac{1}{q(1-q)}}}{\left[\frac{\langle K_\pi \rangle}{\langle K_\mu \rangle} \right]^{\frac{1}{1-q}} + 1} \left[\frac{\langle R_o' \rangle}{\langle K_\pi' \rangle} \right]^{\frac{1}{q}} \qquad (A.2b)$$

Differentiating, one obtains the following partial derivatives:

Run I   Run II

$$\frac{\partial \lambda_I}{\partial \langle K_\pi \rangle} = \frac{\lambda_I}{(1+a)(1-q) \langle K_\pi \rangle} \qquad \frac{\partial \lambda_{II}}{\partial \langle K_\pi \rangle} = \frac{\lambda_{II}(1+a-qa)}{q(1-q)(a+1) \langle K_\pi \rangle}$$

$$\qquad (A.3)$$

$$\frac{\partial \lambda_I}{\partial \langle K_\mu \rangle} = - \frac{\lambda_I}{q(1-q)(1+a) \langle K_\mu \rangle} \qquad \frac{\partial \lambda_{II}}{\partial \langle K_\mu \rangle} = - \frac{\lambda_{II}(1+a-qa)}{q(1-q)(a+1) \langle K_\mu \rangle}$$

Run I   Run II

$$\frac{\partial \lambda_I}{\partial \langle R_o \rangle} = \frac{\lambda_I}{q \langle R_o \rangle} \qquad\qquad \frac{\partial \lambda_{II}}{\partial \langle R_o' \rangle} = \frac{\lambda_{II}}{q \langle R_o' \rangle}$$

$$\frac{\partial \lambda_I}{\partial H} = \frac{\lambda_I}{H} \qquad\qquad\qquad \frac{\partial \lambda_{II}}{\partial H'} = \frac{\lambda_{II}}{H'} \qquad\qquad \text{(A.3 cont'd)}$$

$$\frac{\partial \lambda_{II}}{\partial \langle K_\pi' \rangle} = - \frac{\lambda_{II}}{q \langle K_\pi' \rangle}$$

where $\dfrac{\partial \lambda_I}{\partial H}$ and $\dfrac{\partial \lambda_{II}}{\partial H'}$ reflect the errors in $(p_o)_I$ and $(p_o)_{II'}$, respectively, introduced by uncertainties in the absolute values of the magnetic fields, H and H'.

Let

$$\langle \lambda \rangle = A\lambda_I + (1-A)\lambda_{II} \qquad\qquad (A.4)$$

where A and (1-A) represent the averaging weights of the two measurements λ_I and λ_{II}, respectively.

Differentiating Eq. A.4, substituting in the partial derivatives of Eq. A.3, and assuming $\lambda_I \approx \lambda_{II} \approx \langle \lambda \rangle$, one obtains

$$\frac{\Delta \langle \lambda \rangle}{\langle \lambda \rangle} \approx \frac{\left[A(q-1)(a+1) + (1-q)a + 1 \right]}{q(1-q)(1+a)} \frac{\Delta \langle K_\pi \rangle}{\langle K_\pi \rangle} -$$

$$\frac{1 + (1-q)a}{q(1-q)(1+a)} \frac{\Delta \langle K_\mu \rangle}{\langle K_\mu \rangle} - \frac{1-A}{q} \frac{\Delta \langle K_\pi' \rangle}{\langle K_\pi' \rangle} + \frac{1-A}{q} \frac{\Delta \langle R_o' \rangle}{\langle R_o' \rangle} +$$

$$(1-A) \frac{\Delta H'}{H'} + \frac{A}{q} \frac{\Delta \langle R_o \rangle}{\langle R_o \rangle} + A \frac{\Delta H}{H} \qquad\qquad (A.5)$$

If one now squares Eq. A.5 and takes mean values, the various cross product terms average out to zero. Furthermore, if we now replace

$$\left[\frac{\Delta \langle K_\pi \rangle}{\langle K_\pi \rangle} \right]^2$$

by the experimental variance

$$\frac{\sigma_\pi^2}{n_\pi \langle K_\pi \rangle^2}$$

and the other terms with their corresponding experimental variances, we can write:

$$\overline{\left[\frac{\Delta \langle \lambda \rangle}{\langle \lambda \rangle} \right]^2} = A^2 (a+d) + (1-A)^2 (b+c+e) +$$

$$\left[A (q-1)(a+1) + (1-q) a + 1 \right]^2 f + g \qquad (A.6)$$

where:

$$a = \frac{1}{q^2} \overline{\left(\frac{\sigma_{R_o}^2}{n_o \langle R_o \rangle^2} \right)} \quad , \qquad b = \frac{1}{q^2} \overline{\left(\frac{\sigma_{R_o'}^2}{n_o' \langle R_o' \rangle^2} \right)} \quad ,$$

$$c = \frac{1}{q^2} \overline{\left(\frac{\sigma_\pi'^2}{n_\pi' \langle K_\pi' \rangle^2} \right)} \quad , \qquad d = \overline{\left(\frac{\Delta H}{H} \right)^2} \quad ,$$

$$e = \overline{\left(\frac{\Delta H'}{H'} \right)^2} \quad , \qquad f = \frac{1}{q^2 (1-q)^2 (a+1)^2} \overline{\left(\frac{\sigma_\pi^2}{n_\pi \langle K_\pi \rangle^2} \right)} \quad ,$$

$$\text{and} \quad g = \frac{\left[1 + (1-q) a \right]^2}{q^2 (1-q)^2 (a+1)^2} \overline{\left(\frac{\sigma_\mu^2}{n_\mu \langle K_\mu \rangle^2} \right)} \quad .$$

$$\overline{\left(\frac{\sigma_\pi^2}{n_\pi \langle K_\pi \rangle^2} \right)} \quad , \quad \overline{\left(\frac{\sigma_\pi'^2}{n_\pi' \langle K_\pi' \rangle^2} \right)} \quad \text{etc., now represent the mean square}$$

percentage errors or variances in the quantities $\langle K_\pi \rangle$, $\langle K_\pi' \rangle$, etc., of the individual plates, averaged together for each of the Runs.

Applying the Principle of Least Squares, one differentiates Eq. A.6 with respect to A and sets the derivative equal to zero to find the minimum error in λ . Solving for A, on has

$$A = \frac{b + c + e - (q-1)(a+1)\left[(1-q)\,a + 1\right]\,f}{a + d + b + c + e + (q-1)^2\,(a+1)^2\,f} \tag{A.7}$$

Having obtained this value for A, one then inserts it in Eq. A.4 to give $\langle \lambda \rangle$ and in Eq. A.6 to obtain an estimate of the error.

REFERENCES

1. W. H. Barkas, Meson Mass Measurements I — Theory of the Mass Ratio Method, UCRL-2327 (1953).

2. F. M. Smith, Meson Mass Measurements II — On the Measurement of the Masses of the Charged pions, UCRL-2371 (1954).

3. C. O. O'Ceallaigh, Phil. Mag. 41, 838 (1950).

4. H. Bradner, F. M. Smith, W. H. Barkas, and A. S. Bishop, Phys. Rev. 77, 462 (1950).

5. H. W. Lewis, Phys. Rev. 85, 20 (1952).

6. F. Bloch and A. Nordsieck, Phys. Rev. 52, 54 (1937) among others.

7. H. Primakoff, Phys. Rev. 84, 1255 (1951); Nakano, Nichimura, and Yamaguchi, Prog. Theor. Phys. 6, 1028 (1951); T. Eguchi, Phys. Rev. 85, 943 (1952).

8. W. F. Fry, Phys. Rev. 91, 1930 (1952).

9. For example: G. C. Hanna and B. Pontecorvo, Phys. Rev. 75, 983 (1949); S. C. Curran, J. Angus, and A. L. Cockeroff, Nature 162, 302 (1948).

10. E. Gardner, Private Communication.

11. J. K. Bowker, Privat Communication.

12. A. J. Oliver, Measurements of the Effects of Moisture in Nuclear Track Emulsion, UCRL-2176 (1953).

13. F. Bloch, W. W. Hansen, and M. Packard, Phys. Rev. 70, 474 (1946).

14. R. T. Birge, Phys. Rev. 40, 207 (1932).

15. J. W. M. DuMond and E. R. Cohen, Revs. Modern Phys. 63, 691 (1953).

FIGURE CAPTIONS

Fig. 1. The relation between the π and μ masses for various values
of the neutral particle mass, m_ν, as a function of the abso-
lute decay momentum of the μ meson. This family of curves
shows the extreme sensitivity of the derived neutrino mass to
slight variations of the π/μ mass ratio and the quantity $p_0/m_\mu c$.

Fig. 2. Plan view of the experimental arrangement (Run I) inside the
vacuum tank of the cyclotron. Two typical pion and muon
orbits are shown leaving the target and entering the emulsion
detector.

Fig. 3. Perspective view of the experimental apparatus of Run I. The
target and detector assembly are rigidly mounted on a dural
plate which is fixed in position on the proton probe cart.

Fig. 4. Full-scale drawing of improved target holder of Run II. Back-
ground contamination at detector is reduced to zero.

Fig. 5. Isometric full-scale sketch of plate holder. Fiducial slits
were obtained by photographing a drawing of two sets of
mutually perpendicular lines. The negative of this photo-
graph is glass-backed and is cemented to the inclined brass
surface. The nuclear emulsion detector is fixed in place on
top of the film negative with the aid of the phosphor bronze
leaf springs. A latent image of the fiducial lines is formed
in the emulsion just prior to exposure within the cyclotron.

Fig. 6. Linear measurements of target-detector assembly taken during
Run I. The measurements were obtained with the aid of a
lower power microscope attached to a micrometer traveling
in a direction parallel to that of the Central Radial Line.

Fig. 7. Absolute measurements of the cyclotron magnetic field taken
with the nuclear fluxmeter. Note the change in slope in the
neighborhood of 80 inches.

Fig. 8. Distribution of ranges of μ-completes: 558 events are taken
from 12 plates and normalized to a mean range of 600 microns.
A normal curve fit to the experimental data gives a χ^2-test
significance level of ≈ 0.4.

Fig. 9. Range distributions of μ-completes from five different plates - Run I.

Fig. 10. Pion normalized range distributions from the five plates of Run I. Note the small amount of background. Percentage variance slightly but not signigicantly lower than predicted value. ($R_{1\pi}$ in units of microns and p_π in gauss-mm.)

Fig. 11. Muon normalized range distributions from five plates of Run I showing some contamination. Average percentage variance slightly higher than predicted value. ($R_{1\mu}$ in microns, p_μ in gauss-mm.)

Fig. 12. Pion normalized range distributions from the three plates of Run II. Note the complete absence of any apparent background. Average percentage variance in agreement with prediction. ($R_{1\pi}$ in microns, p_π in gauss-mm.)

Fig. 13. Range distributions of μ-completes from the three plates of Run II.

Fig. 14. Graphical solution to estimate of neutrino mass from Eq. 6. This essentially is an enlarged plot of Fig. 1. The hatched region represents the area subtended by the probable errors in the π/μ mass ratio and the quantity $p_0/m_\pi c$. A probable upper limit of 6-7 m_0 is indicated. ($\beta = m_\nu/m_\mu$)

Fig. 15. Graphical solution to the value of the absolute decay kinetic energy of the muon from the relativistic relation,

$$T_0 = p_0{}^2 c^2 + m_\mu{}^2 c^4 - m_\mu c^2.$$

The hatch region represents the area subtended by the statistical probable errors in m_μ and p_0. The family of curves indicates a value $T_0 = 4.12 \pm 0.02$ Mev.

TABLE I

Summary of mean values of normalized ranges and mu-complete ranges — Runs I and II

	Plate No.	$\left\langle R_{1\pi}P_\pi^{-q}\right\rangle$ $\times 10^{20}$	n_π	$\dfrac{\sigma_\pi}{\left\langle R_{1\pi}P_\pi^{-q}\right\rangle}$	$\left\langle R_{1\mu}P_\mu^{-q}\right\rangle$ $\times 10^{20}$	n_μ	$\dfrac{\sigma_\mu}{\left\langle R_{1\mu}P_\mu^{-q}\right\rangle}$	$\left\langle R_o\right\rangle$	n_o	$\dfrac{\sigma_{R\mu}}{\left\langle R_o\right\rangle}$
Run I	25957	69.82 ± 0.34	31	3.9 ± 0.3%	139.11 ± 1.06	27	5.9 ± 0.6%	596.2 ± 2.8	39	4.4 ± 0.3%
	25958	69.37 ± 0.24	49	3.5 ± 0.2	137.92 ± 0.79	46	5.7 ± 0.4	595.3 ± 2.3	77	4.9 ± 0.3
	25959	70.85 ± 0.25	50	3.6 ± 0.2	140.19 ± 0.62	38	4.1 ± 0.3	593.5 ± 2.4	56	4.4 ± 0.3
	25961	70.68 ± 0.31	51	4.4 ± 0.3	139.49 ± 0.69	30	4.0 ± 0.3	597.6 ± 2.5	50	4.3 ± 0.3
	25967	70.37 ± 0.22	52	3.5 ± 0.2	136.24 ± 0.98	20	4.8 ± 0.5	598.7 ± 3.1	53	5.6 ± 0.4
Run II	28848	70.84 ± 0.22	69	3.8 ± 0.2				599.0 ± 2.8	26	3.6 ± 0.3
	28849	72.48 ± 0.22	71	3.7 ± 0.2				605.6 ± 3.3	31	4.6 ± 0.4
	28853	70.74 ± 0.24	78	4.5 ± 0.2				593.4 ± 3.1	32	4.5 ± 0.4

$R_{1\pi}$, $R_{1\mu}$, and R_o in units of microns

p_π and p_μ in units of gauss-mm

$\sigma_{R\mu}$ is the observed straggling of the mu-completes, uncorrected for the "staying-in" probability of the tracks (see Sec. V A, Paper II)

All errors quoted are statistical probable errors

TABLE II

Summary of calculation of pi-mu mass ratio

Plate No.	α'	α	Probable error (p. e.) in α
25957	1.326_4	1.325_8	$\pm 0.004_9$
25958	1.325_3	1.326_5	$\pm 0.003_6$
25959	1.322_7	1.320_5	$\pm 0.003_0$
25961	1.321_3	1.322_0	$\pm 0.003_6$
25967	1.311_0	1.307_9	$\pm 0.004_3$

α' = apparent mass ratio

α = mass ratio corrected for finite target-detector and Lewis effects

Weighted Mean: $\alpha = 1.321 \pm 0.002$

Probable Error – Internal Consistency = $\pm 0.001_7$

Probable Error – External Consistency = $\pm 0.002_0$

TABLE III

Summary of calculations of absolute decay momentum

Run	Plate No.	P_o' x 10^{-5}	P_o x 10^{-5}	Statistical p.e.* in P_o x 10^{-5}
I	25957	9.946	9.954	± 0.026
	25958	9.967	9.961	± 0.020
	25959	9.911	9.930	± 0.017
	25961	9.945	9.943	± 0.019
	25967	10.019	10.046	± 0.026
II	28848	9.947	9.948	± 0.016
	28849	9.913	9.912	± 0.018
	28853	9.924	9.924	± 0.018

* Does not include uncertainty in absolute value of magnetic field

P_o' = apparent value of absolute decay momentum in gauss-mm

P_o = value of absolute decay momentum corrected for finite target-detector and Lewis effects

Run I: Weighted Mean = 9.958 x 10^5 gauss-mm

        Statistical Probable Error — Internal Consistency = ±0.009 x 10^5

        Statistical Probable Error — External Consistency = ±0.011 x 10^5

$\langle P_o \rangle_I$ = 29.85 ± 0.05 Mev/c (including uncertainty in absolute magnetic field)

Run II: Weighted Mean = 9.929 x 10^5 gauss-mm

        Statistical Probable Error — Internal Consistency = ±0.010 x 10^5

        Statistical Probable Error — External Consistency = ±0.007 x 10^5

$\langle P_o \rangle_{II}$ = 29.77 Mev/c (including uncertainty in absolute magnetic field)

Figure 1

MU-1707

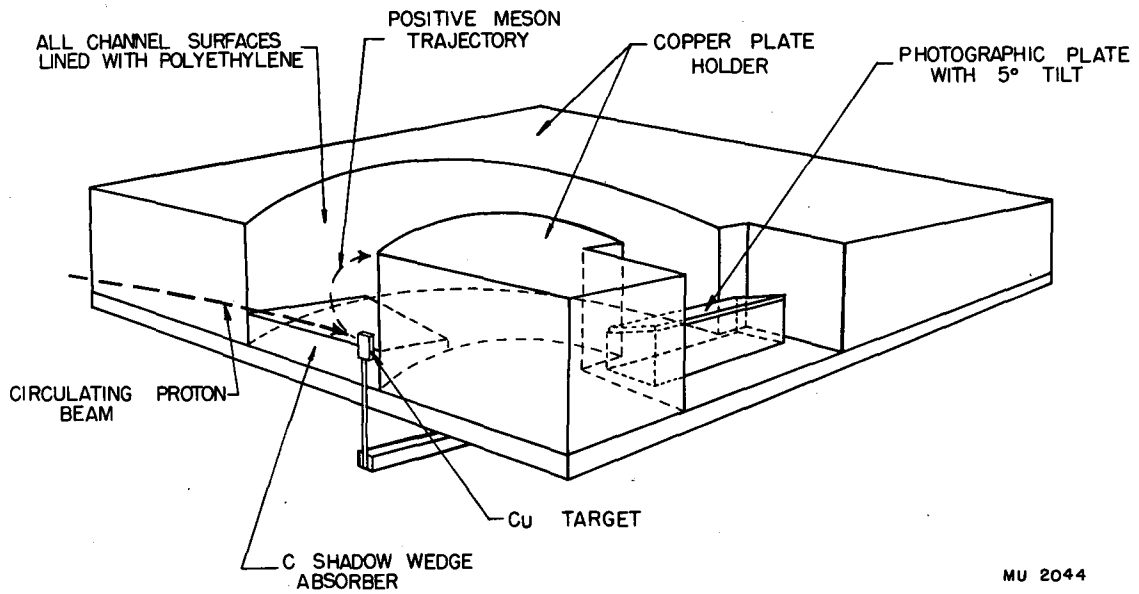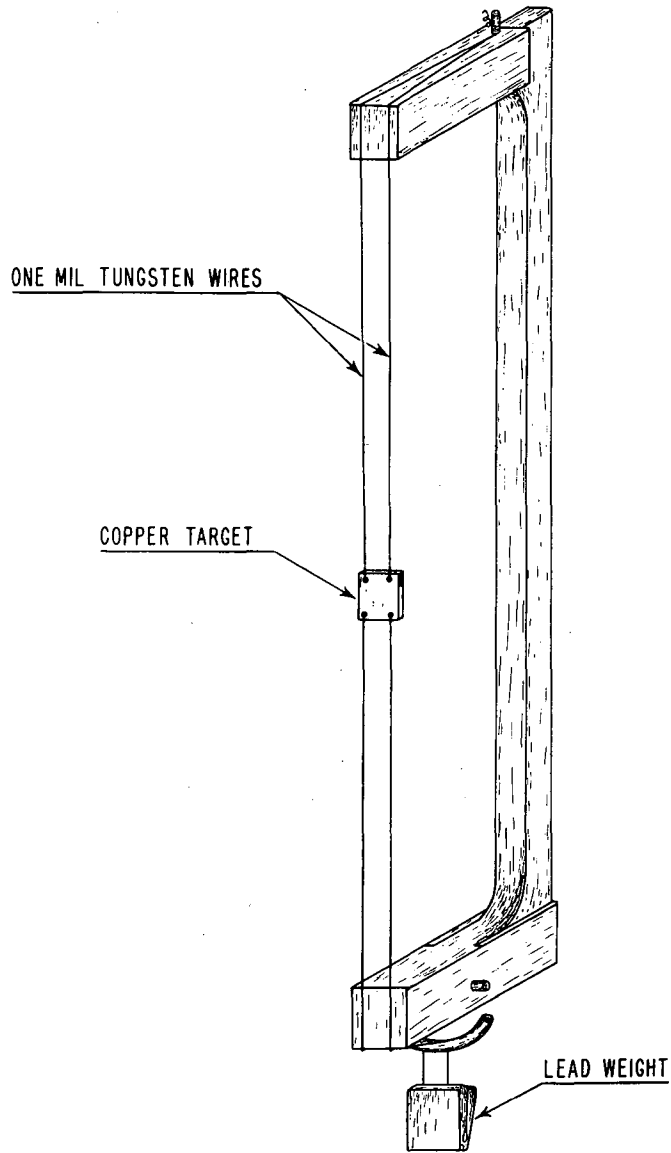PLATE   HOLDER π^+/μ^+ MASS   RATIO - PLAN VIEW
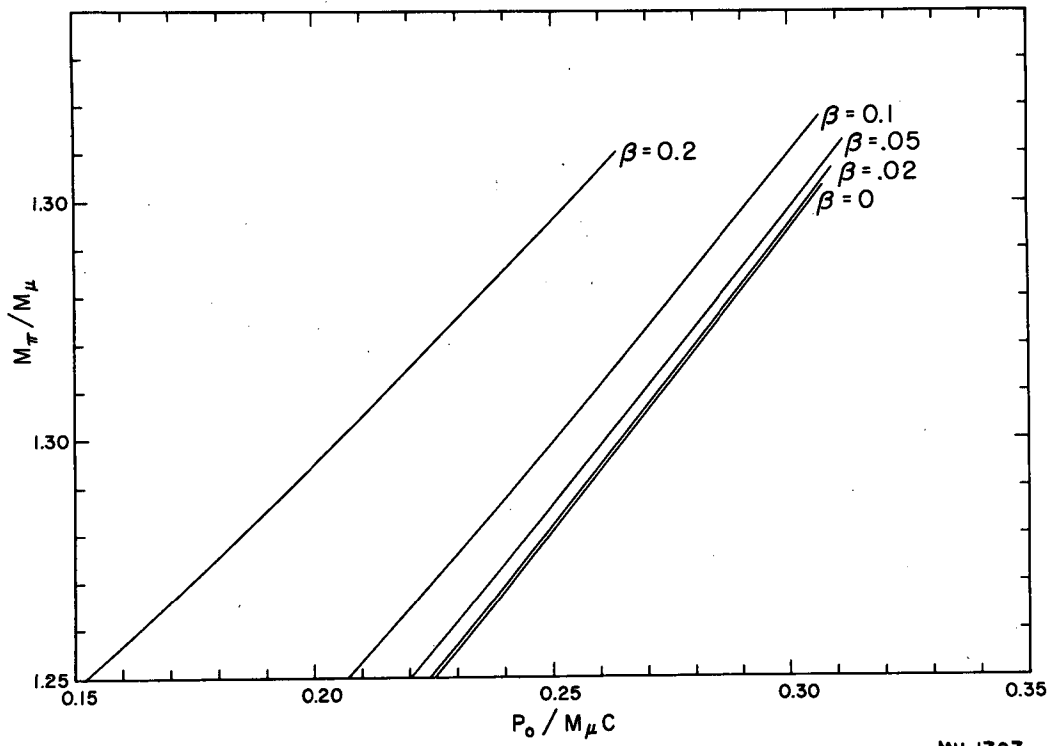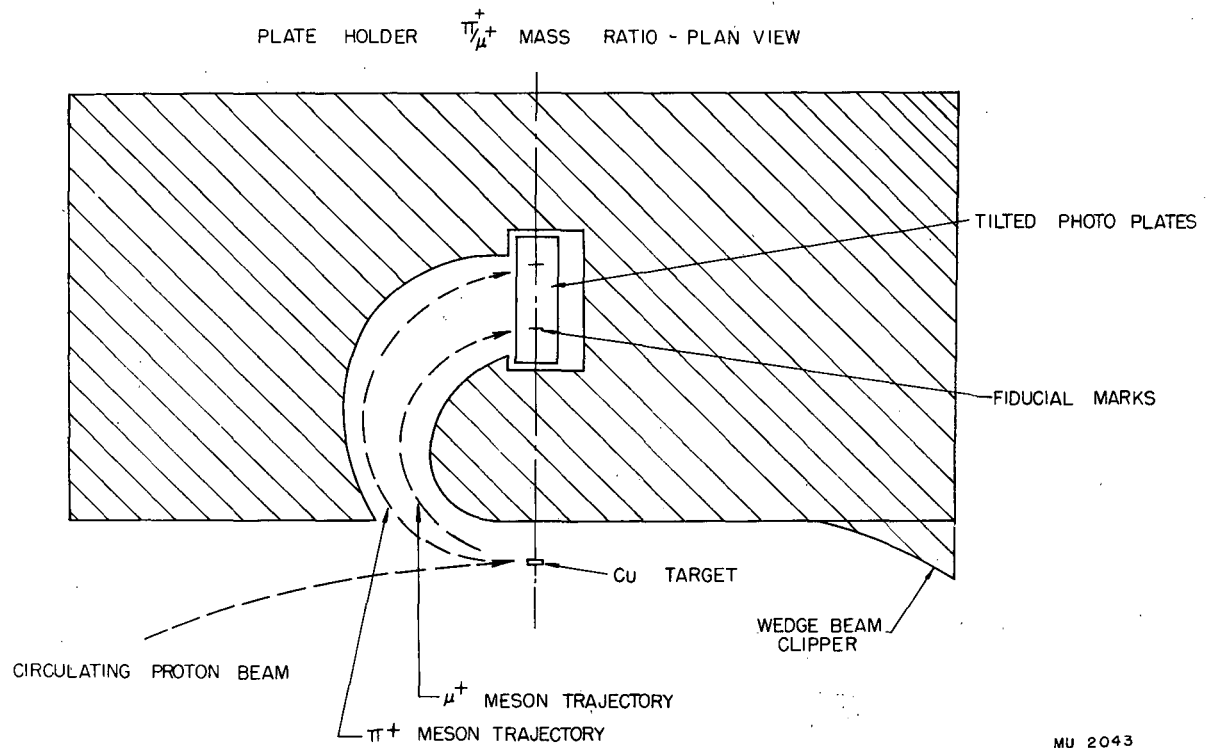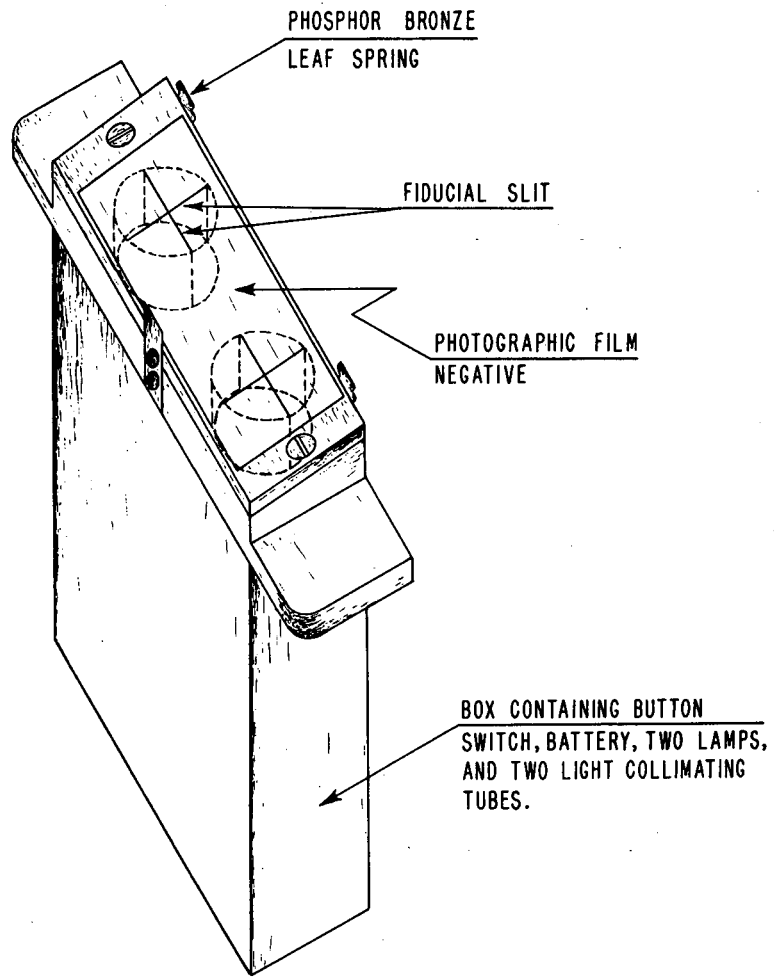

Figure 2

PLATE   HOLDER $^\pi/_\mu$ MASS RATIO EXPT.

Figure 3

ONE MIL TUNGSTEN WIRES

COPPER TARGET

LEAD WEIGHT

MU-7205

Figure 4

PHOSPHOR BRONZE
LEAF SPRING

FIDUCIAL SLIT

PHOTOGRAPHIC FILM
NEGATIVE

BOX CONTAINING BUTTON
SWITCH, BATTERY, TWO LAMPS,
AND TWO LIGHT COLLIMATING
TUBES.

MU-7206

Figure 5

Figure 6

Figure 7

$\langle R_o \rangle$= 600 MICRONS

$\frac{\sigma_{R_o}}{\langle R_o \rangle}$ = (4.5$_3$ ± 0.1$_4$) %

SKEW $\frac{\beta_3}{\beta_2^{3/2}}$ =

0.03 ± 0.12

OBSERVED

NORMAL CURVE FIT

NUMBER OF EVENTS

RANGE IN MICRONS
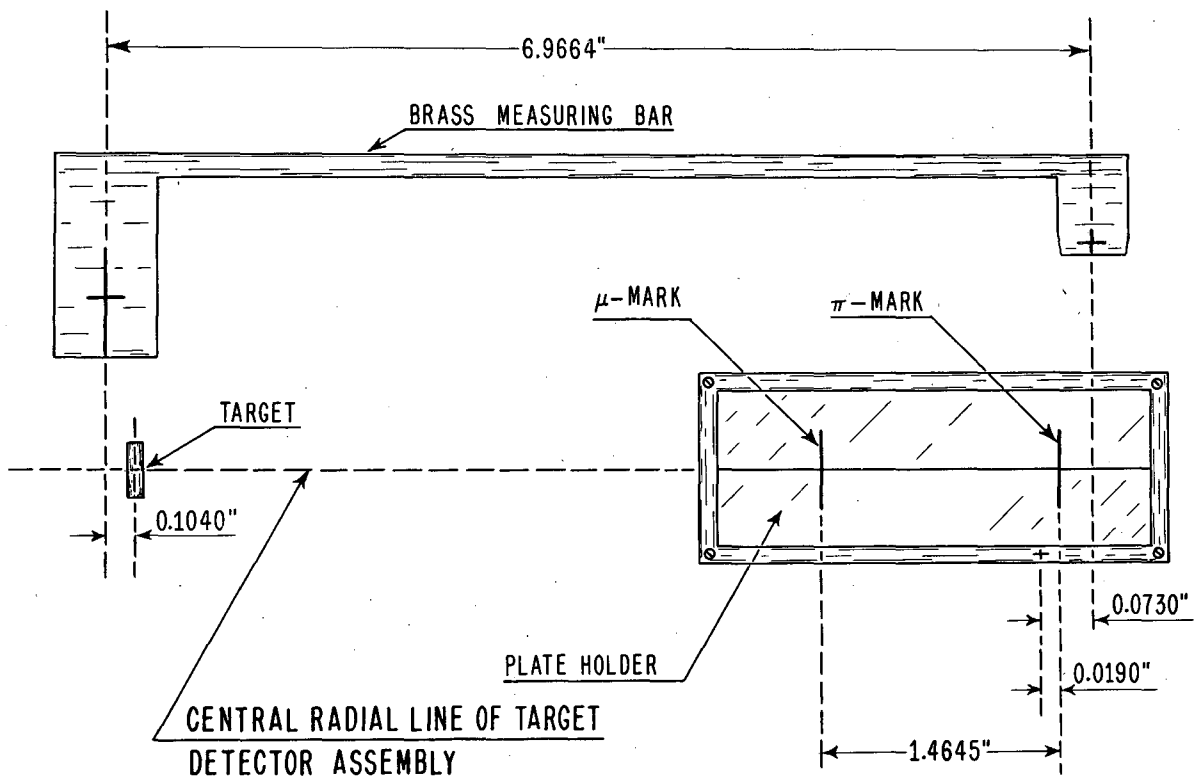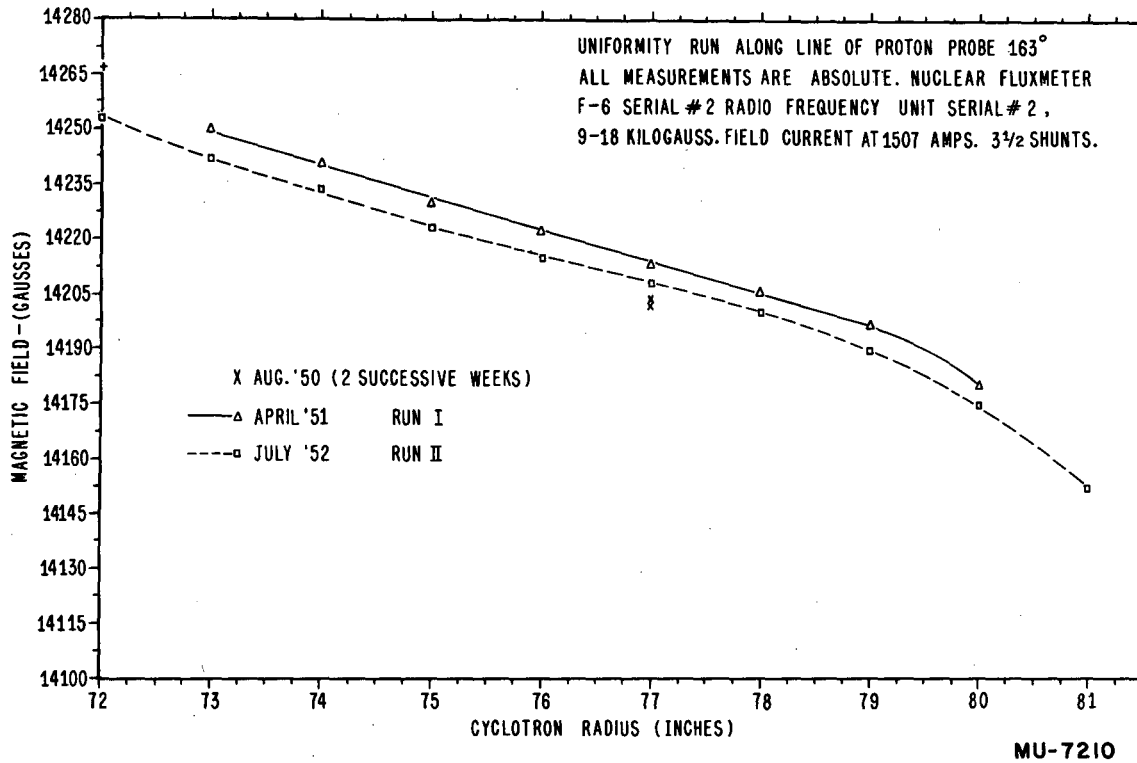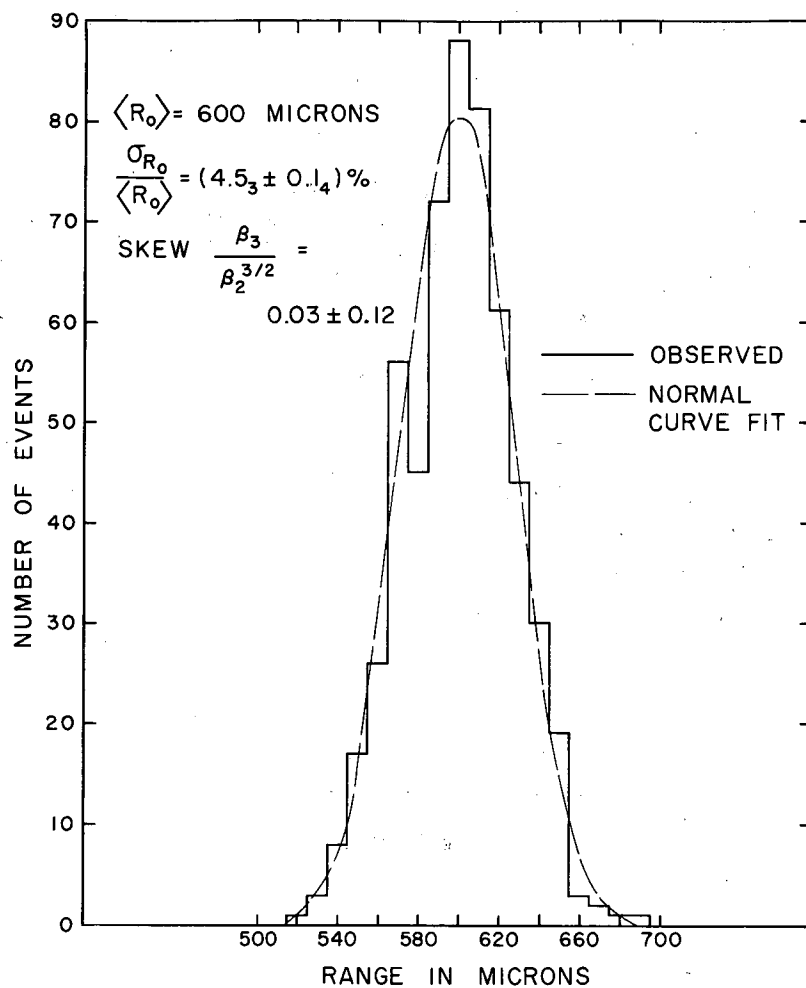
MU-6968

Figure 8

Figure 9

Figure   10

Figure 11
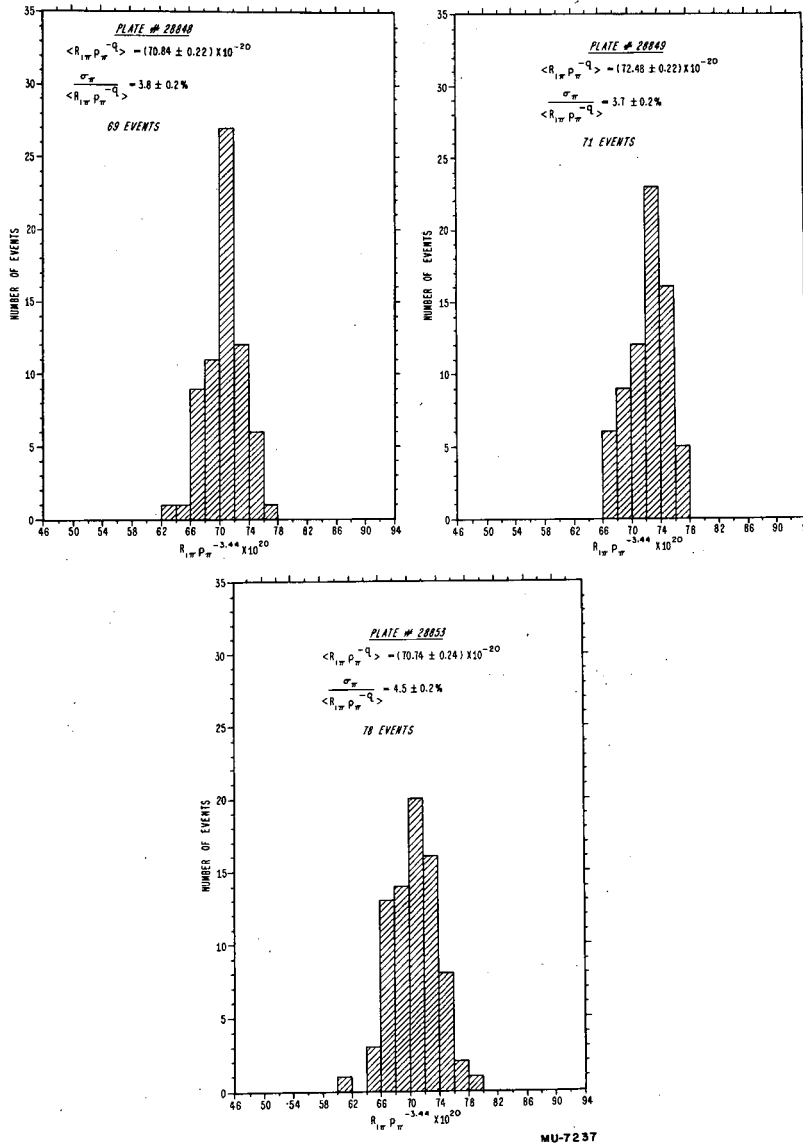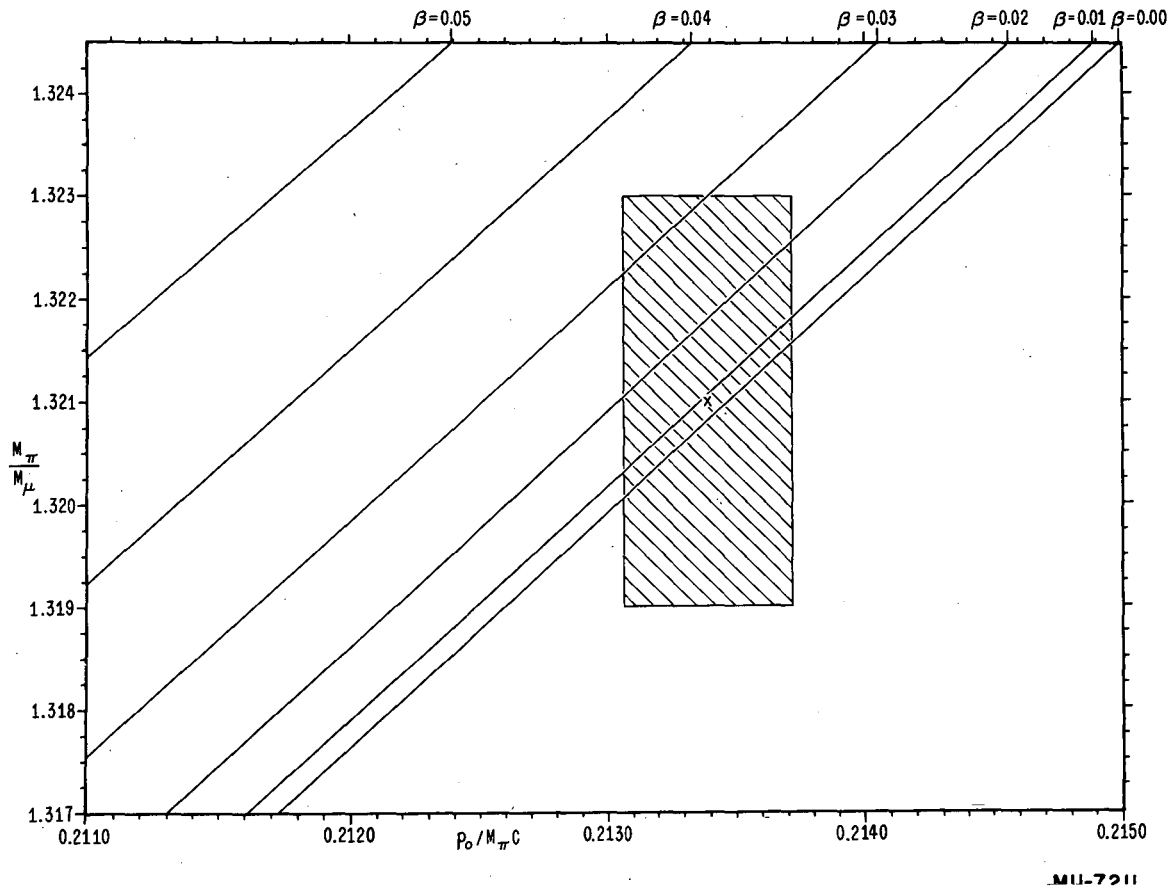
MU-7236

Figure 12

PLATE # 28848
$<R_o> = 599.0 \pm 2.8$ MICRONS
$\dfrac{\sigma_{R_\mu}}{<R_o>} = 3.6 \pm 0.3 \%$
26 EVENTS

PLATE # 28849
$<R_o> = 605.6 \pm 3.3$ MICRONS
$\dfrac{\sigma_{R_\mu}}{<R_o>} = 4.6 \pm 0.4 \%$
31 EVENTS

PLATE # 28853
$<R_o> = 593.4 \pm 3.1$ MICRONS
$\dfrac{\sigma_{R_\mu}}{<R_o>} = 4.5 \pm 0.4 \%$
32 EVENTS
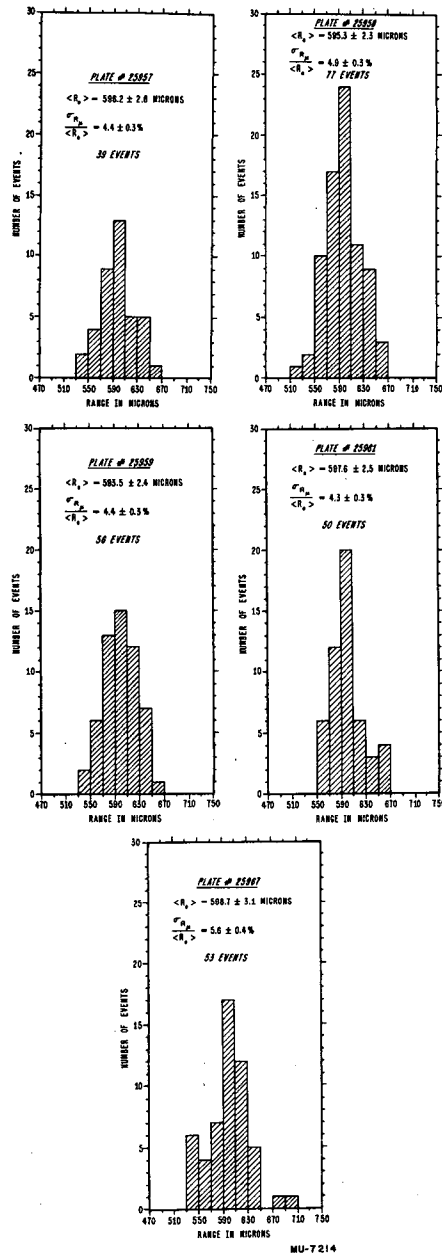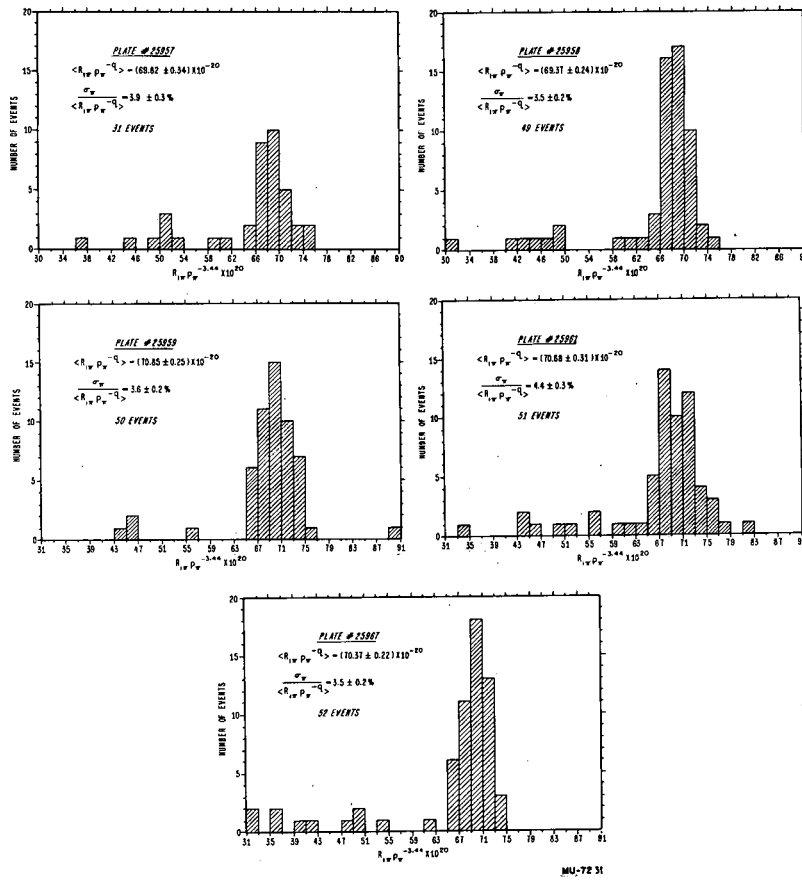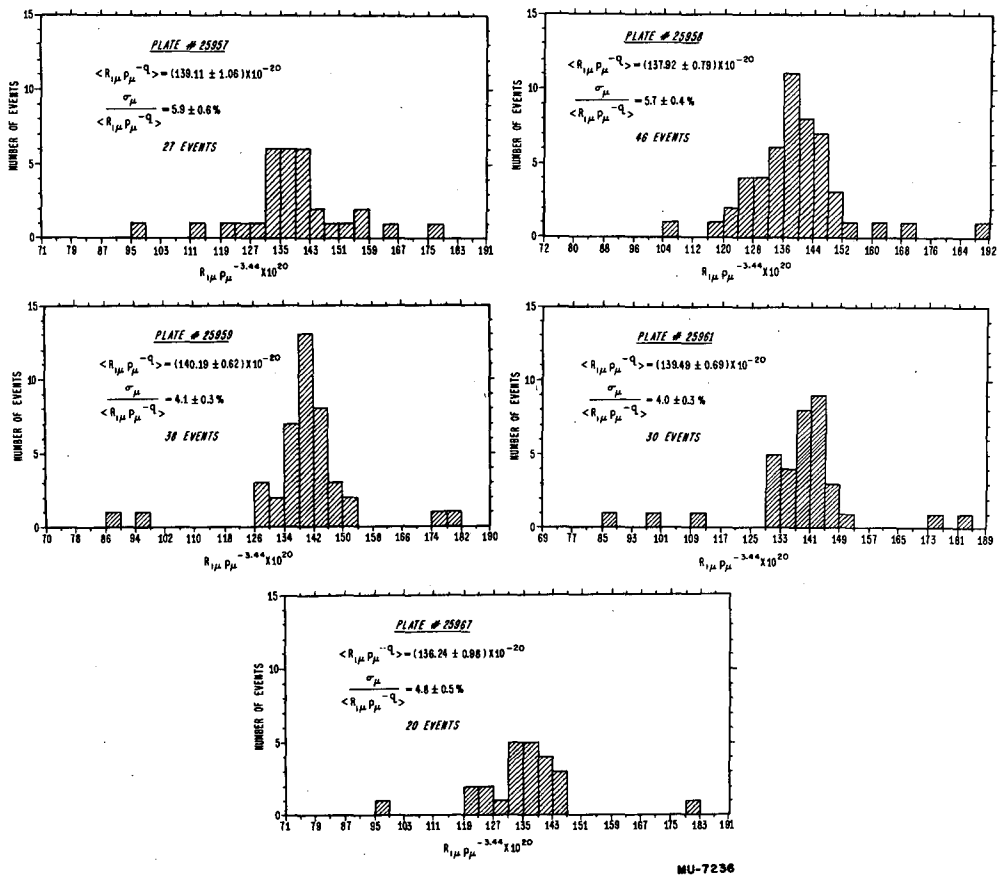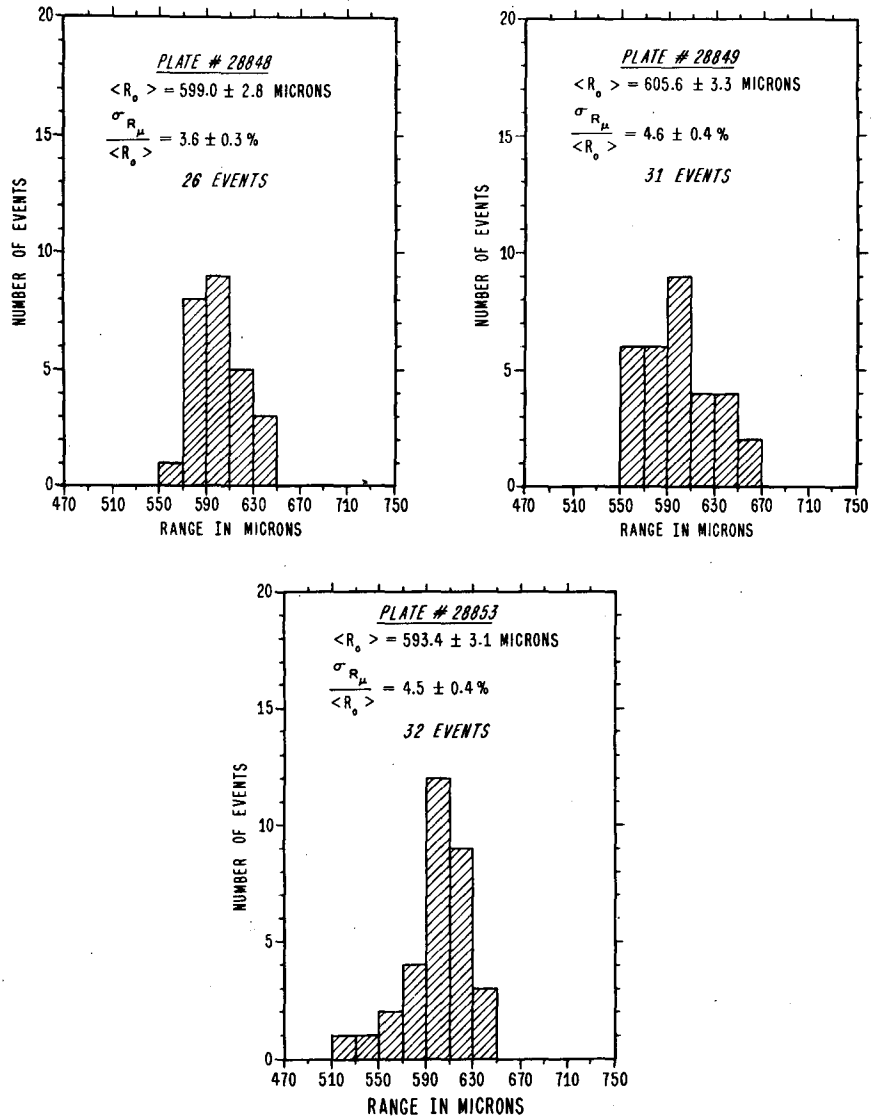
MU-7213

Figure 13

Figure 14

Figure 15